Original

Lehmann, J.; Chen, H.; Kruse, M.; Ben Khalifa, N.:
Introducing Residual Stresses on Sheet Metals by Slide Hardening under Stress Superposition.
In: Key Engineering Materials. Vol. 883 (2021) 143 - 150.

First published online by Trans Tech Publications: 27.04.2021

https://dx.doi.org/10.4028/www.scientific.net/KEM.883.143

Key Engineering Materials
ISSN: 1662-9795, Vol. 883, pp 143-150
doi:10.4028/www.scientific.net/KEM.883.143

Submitted: 2020-10-15
Revised: 2020-11-20
Accepted: 2020-12-04
Online: 2021-04-27

Introducing Residual Stresses on Sheet Metals by Slide Hardening under Stress Superposition

Jonas Lehmann[1,a*], Hui Chen[1,b], Moritz Kruse[1,c] and Noomane Ben Khalifa[1,2,d]

[1]Leuphana University of Lüneburg, Institute of Product and Process Innovation, Universitätsallee 1, 21335 Lüneburg, Germany

[2]Helmholtz-Zentrum Geesthacht, Institute of Materials Research, Max-Planck-Str. 1, 21502 Geesthacht, Germany

[a]jonas.lehmann@leuphana.de, [b]hui.chen@leuphana.de, [c]moritz.kruse@leuphana.de, [d]noomane.ben_khalifa@leuphana.de

*corresponding author

Keywords: Hardening, Residual stress, Stress superposition

Abstract. The fatigue strength and product life of the components can be improved by introducing compressive residual stresses using mechanical surface treatment. Appling stress superposition is an option to be used in metal forming to reduce the process force. In this work experimental investigations to analyze the influence of stress superposition on residual stresses of sheet metal parts by a slide hardening process were carried out. The flat and elastically pre-bended specimens (i.e. stress-superimposed specimen) were processed with a slide diamond tool under different loading forces. The residual stress generated through the thickness of the sheet metal was similar for the flat and the pre-bended specimens. The superimposed stress by elastic bending of the sheet metal led to higher compressive residual stress compared to the flat specimen under the same loading force. Nevertheless, the contour of the pre-bended specimen showed more bulking compared to the flat specimen. The mechanical characteristics determined by hardness measurements showed no significant improvement when applying stress superposition.

Introduction

Wear and tear cause high resource consumption in the transportation and manufacturing industry. To reduce this, it is necessary to improve the macro-characteristics in the boundary layers and the micro-characteristics in the surface and sub-surface layers. For this purpose, there are different strain hardening treatment techniques, which increase the strength and product life of components and make lightweight construction possible.

There are more than six surface engineering treatment methods on aluminium alloy AA2024-T3 [1]. Well known methods are Shot Peening (SP), Laser Shock Peening (LSP) and Deep Rolling (DR) [2]. After SP a further surface treatment method is necessary to reduce surface roughness [3]. LSP is established in the aviation industry and leads to retardation of fatigue crack propagation as well as closure of small cracks [4]. LSP generates hardening by cold working [5] and leads to no surface improvement [3].

DR generates higher compressive residual stress and strain hardening than LSP near the surface and smooths the surface [3]. Due to work hardening, DR increases the microstructural dislocation density and hardness of the surface layers. Compressive residual stresses increase the fatigue strength and improve crack growth. Surface smoothing by the tool results in a reduction of micro notches and lower sliding friction.

Considering the shape of the deforming element, there is a difference between roller and balls [6]. Moreover, there are distinctions of the contact type between deforming tool and workpiece by rolling and sliding. Maximov et al. [7] induced a plastic deformation by a tool with a spherical diamond tip in surface layers of AA2024-T3 Al alloy bar stock and called it slide diamond burnishing (SDB). Some research applied mechanical surface treatment to rotating cylindrical workpieces to burnish the part surface. For surface treatment of plane specimens, multi-axis tool feed were conducted [6]. Most

publications investigated inducing residual compressive stresses by mechanical surface treatment for bulk metal, while less research for sheet metal was mentioned.

Loading force of the burnishing tools was needed to induce plastic deformation on the contact area of the workpieces. An ultrasonic vibration accompanied ball burnishing process showed the feasibility of improving surface quality and achieving residual stresses with lower loading force [8]. Stress superposition was intently used to reach additional plastic deformation of the material to extend the forming limits or to reduce process forces [9].

The aim of this work is to investigate the effect of stress superposition on residual stress generation in slide diamond hardening (SDH). In SDH, a slide diamond tool is used in a surface treatment process similar to deep rolling for applying residual stresses in sheet metal part, i.e. AA2024-T3 sheet in this research. The residual stresses that were determined by hole drilling methods are compared between experiments with and without stress superposition applied by pre-bending of the sheet material. In addition to residual stresses, the specimen deformation is shown to discuss the results and hardness measurements are compared to demonstrate the effect of work hardening under stress superposition.

Experimental Procedure

Material and Stress Superposition. The experimental specimens are aluminium sheet AA2024-T3 used in aviation industry. Mechanical material data are summarized in Table 1. The specimen geometry of the sheet material is 60 x 40 mm with a thickness of 2 mm. Fig. 1a shows the specimen geometry without prestress. Fig. 1b shows the same specimen geometry in the bended state for experiments with stress superposition. Stress superposition was realized by elastic pre-bending caused by the specimen holder. Fig. 2 shows the stress state occurring during elastic bending. The bending induces tensile stresses on one and compression stresses on the other side of the sample with values being highest close to the surface.

Table 1: Mechanical material data of aluminium sheet AA2024-T3

Young's Modulus E	Yield stress $R_{p0.2}$
71100 [N/mm²]	325 [N/mm²]

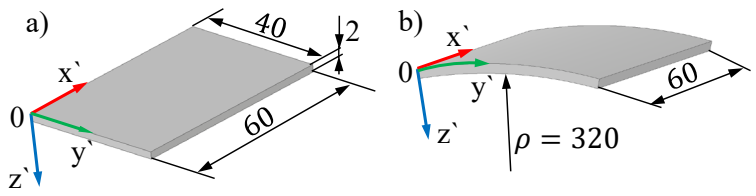

Fig. 1: Specimen geometry a) without prestress, b) with elastic bending

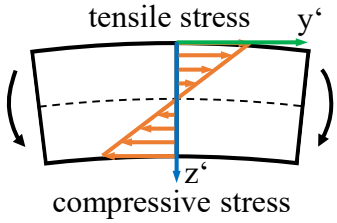

Fig. 2: Stress state during elastic bending

The maximum stress, i.e. the stress at the surface of the blank can be calculated with Eq. 1 according to Marciniak [10]:

$$\sigma_1 = E \frac{y}{\rho}. \quad (1)$$

The distance y from the neutral axis is 1 mm. According to the mechanical material data (Table 1) the radius of the specimen holder ρ = 320 mm results in an elastic bending with 68 % yield stress (σ_1).

Slide Diamond Hardening Process. A 5-axis milling portal with Siemens Computerized Numerical Control (CNC) was used for the experimental process setup. Fig. 3 shows the experimental process setup consisting of a spring loaded tool with spherical diamond tip in the tool holder of the machine, the specimen in the specimen holder and a force measurement plate. The slide diamond

burnishing tool (Baublies AG) is designed for smoothing surfaces as well as for work hardening and induction of compressive residual stress. Process parameters can be taken from Table 2.

The surface treatment area and the process path strategy are shown in Fig. 4. After processing the front side (side A), the sheet metal parts were flipped so that the backside (side B) of the sheet metal could be processed afterward. The long processing path direction is parallel to the material rolling direction. The *y* and *z* coordinate had to be adjusted for the curved specimen under bending. For comparing bended specimens with flat specimens, the tool should be perpendicular to the specimen. In case of small bending the curvature of the surface is so small that an adjustment of the tool angle can be neglected in this experimental setup.

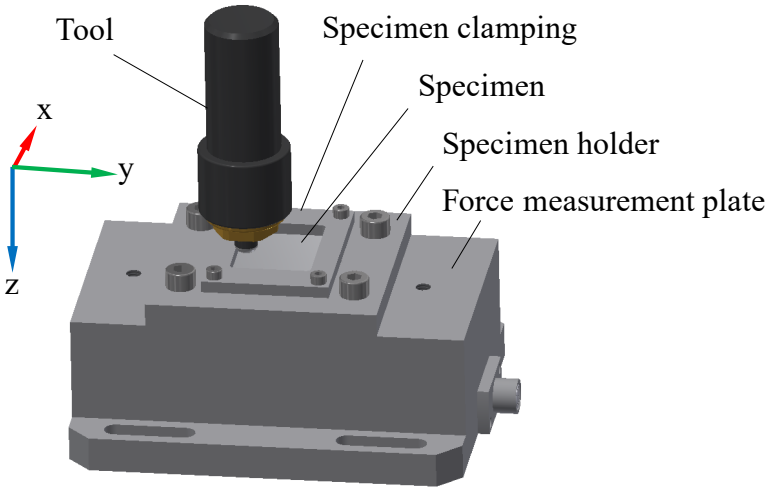

Fig. 3: Experimental setup

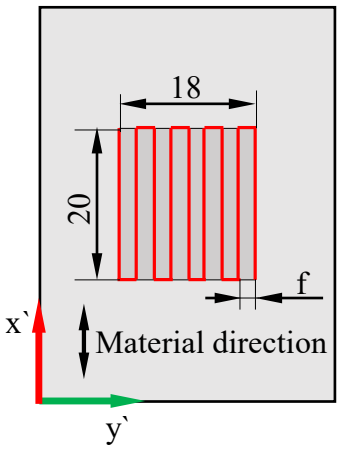

Fig. 4: Processing area and process path strategy

In Table 3 the experimental design is listed. Both flat and bended specimens were tested at four different loading forces. The force was controlled by the *z* feed. A force sensor below the specimen holder measured the forces occurring in the process. The force sensor is a multi-component dynamometer up to 10 kN from Kistler. When processing the curved specimen, the height in *z* direction had to be readjusted so that the force remains constant in the process. Fig. 5 shows the force curves in the SDH process. A constant force curve in *z* direction was achieved by adjusting the tool height with half of the specimen holder radius.

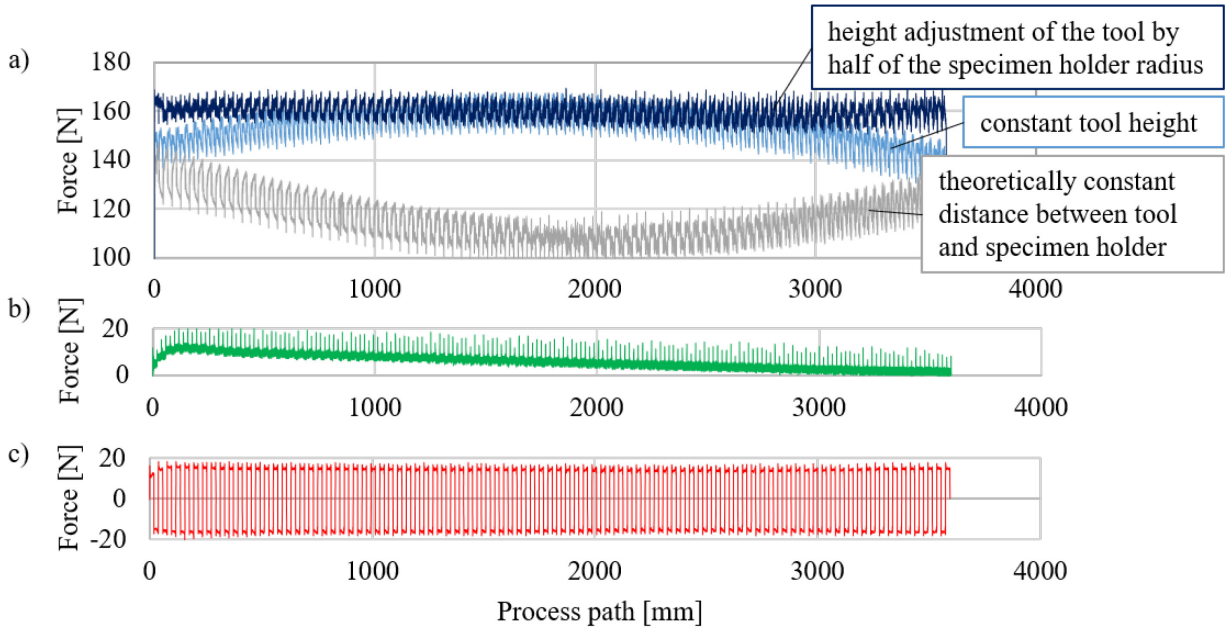

Fig. 5: Process forces when processing a specimen under bending in a) *z* direction b) *y* direction and c) *x* direction

Table 2: Process parameters of SDH

Tool diameter diamond ball	8 [mm]
Process path distance f	0.1 [mm]
Process speed	500 [mm/min]
Number of overruns	1
Processed specimen sides	both sides
Lubrication	oil

Table 3: Experimental design

	Specimen flat	Specimen under bending
Loading force	40 [N]	40 [N]
	70 [N]	70 [N]
	150 [N]	150 [N]
	190 [N]	190 [N]

Residual Stress Analysis. An incremental hole drilling method system (Prism, Stresstech) was used to determine the residual stress. While the maximum analyzable depth is limited for x-ray, the hole drilling method determines compressive residual stresses up to a depth of 2 mm [11]. The procedure of the measurement follows the sequence: (1) drilling a hole in the processed area; (2) measuring the material deformation by electronic speckle pattern interferometry; (3) calculating the residual stress [12].

The diameter of the used driller is 2 mm and the specimens were tested with 1 mm distance from both sides to the neutral plane of the sheet metal. The holes were drilled in the processed area with sufficient distance to the side edge, so that the determined residual stresses represent the area of surface treatment. Measurements were taken at different locations.

The measuring system assumes pure elastic deformation, which may explain residual stress values above the yield stress [13]. High values may be quantitively flawed but qualitatively correct. This has to be taken into consideration when interpreting the results.

Contour Measurement. A three-dimensional scanner (GOM ATOS) was used to perform measurements to capture the specimen contour in the *y*-*z*-plane in different process stages. Two *x'* locations for a specimen with and without stress superposition were chosen. The first measurement was taken in the middle of the specimen and treated area ($x' = 30$). The second measurement was taken at $x' = 10$ outside of the treated area.

Hardness Measurement. The Brinell hardness HBW 2.5/15.625 according to DIN EN ISO 6506-1 was measured at the processed area.

Results and Discussion

Residual Stress. The residual stresses in *x* and *y* direction are shown in Fig. 6 for the representative specimens processed with a loading force of 70 N with and without stress superposition. The surface treatment produces compressive residual stresses near the surface of the specimens as intended, due to the plastic deformation of the material. A similar stress pattern is achieved in *x* and *y* direction. The flat specimen shows the same residual stresses for both processed sides and also in *x* and *y* direction. However, the specimens processed with stress superpositions show higher residual stresses in both *x* and *y* direction. This implies that stress superposition can be used to lower process forces for achieving the same residual stresses in a part.

The residual stress pattern for the flat and bended part is different. A tensile residual stress is presented at the very near surface of the bended specimen. At a thickness depth of 0.2 mm, a maximum compressive stress appears. The compressive residual stress decreases until tensile residual stress presents close to the neutral plane of the sheet metal part. In the flat specimen, the compressive stress was initiated in the very near surface of the specimen, while compressive stress decreases throughout the thickness direction. The pattern of the stress distribution of the flat specimen with 70 N process force is similar to both the flat and bended specimen with 40 N process force. For the bended specimen with 70 N process force the pattern is similar to the experiments under higher loading forces (150 N and 190 N) for both bended and flat specimens.

Fig. 7 shows a comparison between the bended specimen with a force of 70 N and a flat specimen with a force of 150 N. It is noticeable that the residual stresses in *x* direction show the same pattern

and amplitude for the first processed side (side A), while the stresses in *y* direction have the same pattern as well with only slightly higher values. This indicates that stress superposition can not only be applied for achieving higher residual stress values with a significantly lower force but that also the pattern and therefore the properties of the manufactured part is similar to when using higher forces and no stress superposition.

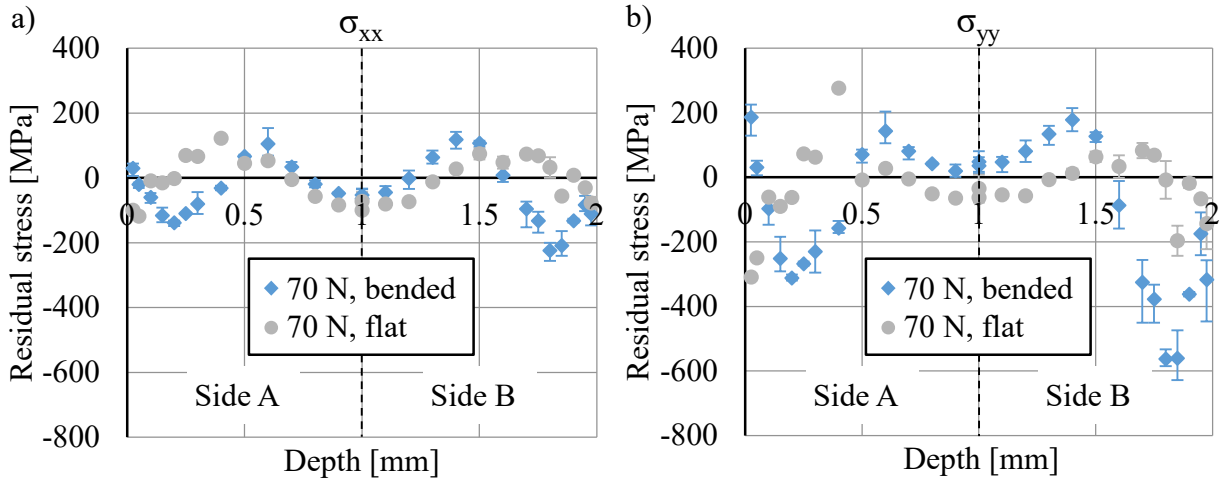

Fig. 6: Comparison of residual stresses in a) *x* and b) *y* direction through the thickness of the specimen for a loading force of 70 N with and without stress superposition.

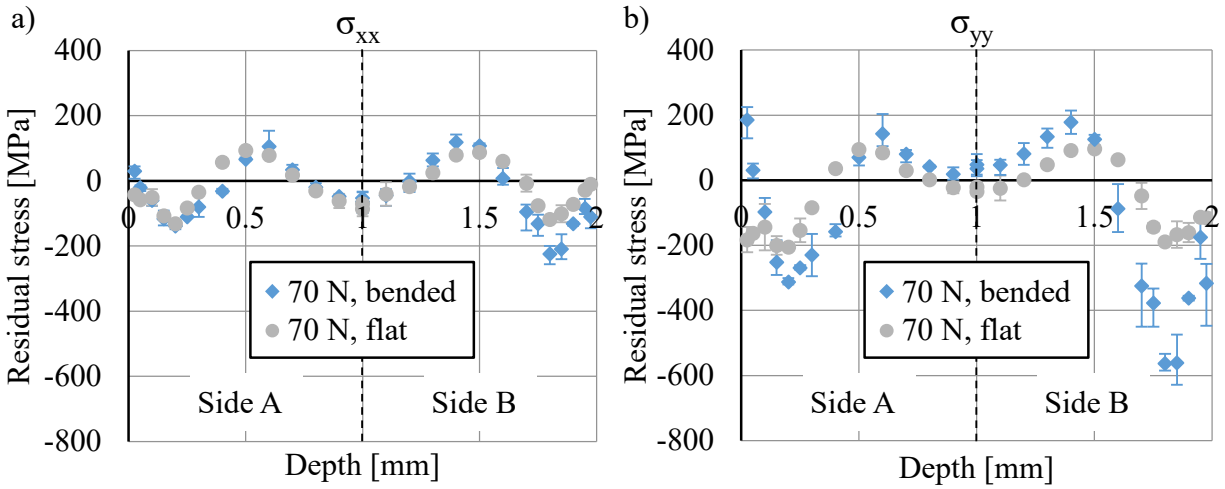

Fig. 7: Comparison of residual stresses in a) *x* and b) *y* direction through the thickness for a specimen processed with 70 N in a flat state and a specimen processed with 150 N in a bended state.

Fig. 8 shows a comparison of the compressive residual stresses in *x* and *y* direction as well as a comparison of side A and side B for all tested specimens processed with different forces. For this purpose, an integral for negative residual stress values was calculated by connecting the measurement points and summing up the areas under the curve. Fig. 8a shows the comparison of stresses in *x* and *y* by using the mean of side A and side B, while for figure 8b the mean of stresses in *x* and *y* direction were plotted for showing the differences between side A and B. As expected, a higher loading force leads to higher residual stresses in the material with and without stress superposition. Residual stresses in *y* are higher than in *x* direction for the flat and bended specimen. This might be due to the raw sheet material being anisotropic for example because of the rolling. When comparing the bended 40 N specimen and the flat 150 N specimen, similar residual stresses in *x* were measured. In *y* direction though, the residual stresses in the bended specimen are higher than in the flat specimen. This implies that residual stresses in *y* direction were induced during SDH through bending of the material in that same direction. In general, Fig. 8 as well displays that higher residual stresses could be achieved when applying stress superposition.

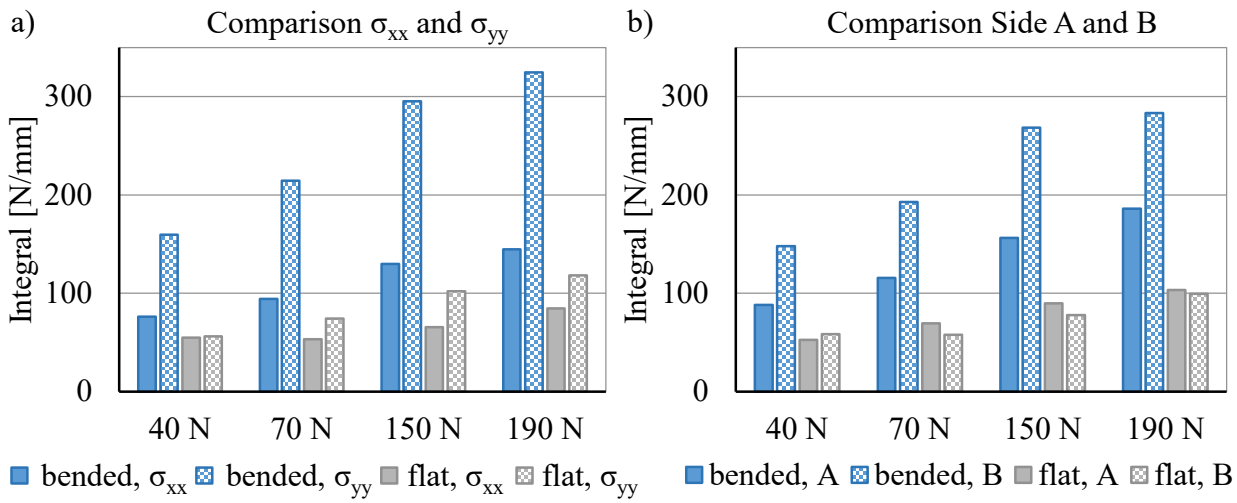

Fig. 8: Comparison of the integral of compressive residual stresses for each specimen in a) *x* and *y* direction and b) for side A and B under different forces.

Stress superposition also leads to higher residual stresses on the processed backside (side B) of the specimen. This might be due to having not only elastic deformation after the first bending but also plastic deformation due to the SDH process of the first side. The reverse bending leads to greater pre-stress than the calculated 68 % yield stress and therefore plastic deformation.

Contour Deformation. To inspect contour deformation, geometry measurements of side A of the specimen were performed at different process stages. Fig. 9 shows buckling of the specimen measured before and after SDH on first and second side.

After SDH side A a displacement of up to 0.2 mm was measured, which indicates plastic deformation of the sample due to stress superposition of bending stress and stresses induced by the SDH force. The flat sample in comparison had little buckling after processing the first side (around 0.05 mm or 2.5 % of the sample thickness). Plastic deformation therefore occurs due to SDH alone as well but is increased by the bending of the specimen.

The measurements outside the treated area (*x'* = 10 mm) show smaller deformations which also indicate that plastic bending of the specimen is induced by processing.

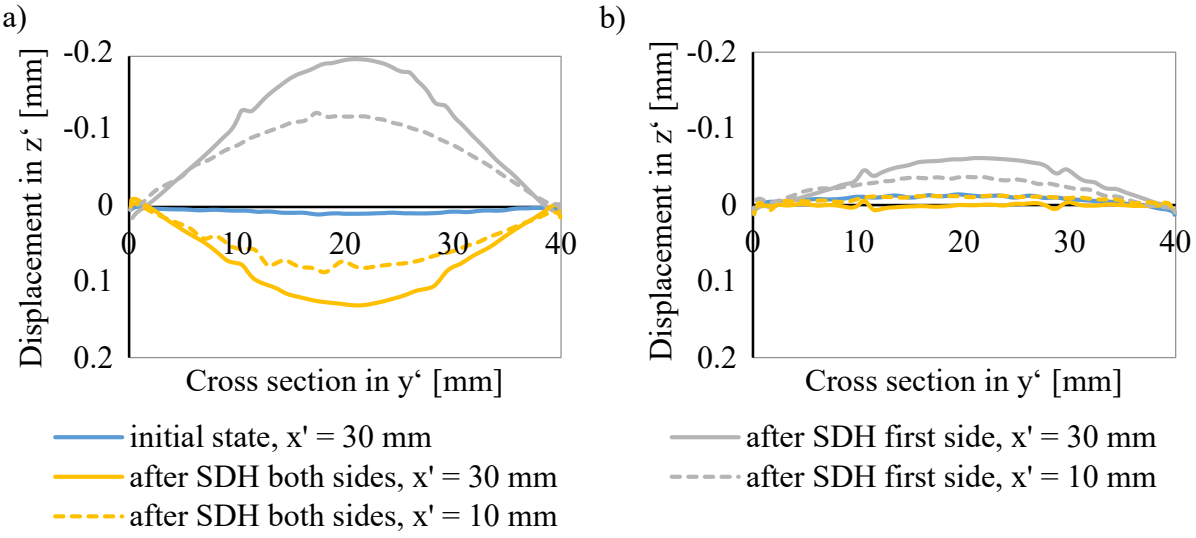

Fig. 9: Deformation of side A in *y*-*z* plane at different process stages and positions *x'* = 10 mm and *x'* = 30 mm a) for a specimen processed with stress superposition and b) without stress superposition, both with a force of 190 N.

After SDH the second side of the bended specimen, the permanent displacement reversed and also decreased to about half the value because of the reverse bending. The flat specimen however showed no displacement anymore after processing the second side. Because of having permanent plastic deformation after SDH the first side, the reverse bending alone might induce plastic deformation in the other direction which changes the stress state before and after SDH the second side. Possibly the Bauschinger effect also has an influence on that [14].

Brinell Hardness Measurement. The hardness measurements in Fig. 10 show slightly higher hardness values for the bended specimens, but not for all forces. This might mean that applying stress superposition can increase surface hardness. Hardness does not significantly differ in the flat specimens for forces above 70 N. For 190 N, the hardness is even slightly lower than for 150 N.

Thus, while compressive residual stresses do increase with higher SDH force and stress superposition, surface hardness does not increase with higher SDH forces after a threshold. This might imply that a part of the higher residual stresses come from the plastic deformation due to SDH. Hardness is not significantly different on side A and B of the specimens although the results show a tendency of side A having higher hardness.

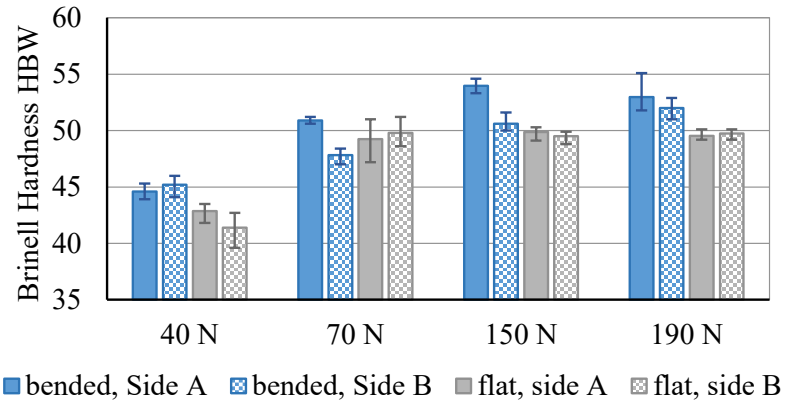

Fig. 10: Brinell Hardness measurements for each side of every specimen

Summary

In this paper, the influence of stress superposition on surface treatment processes were investigated. For this, AA2024-T3 specimens were treated with a slide diamond tool while applying stress superposition by elastic bending of the specimen. Residual stresses, hardness and plastic deformation were analyzed. It was shown that the same residual stress values and distributions could be achieved with lower process forces when implementing stress superposition. Residual stresses on the second processed side are higher than on the first processed side. This might be due to reverse bending of the specimens and plastic deformation occurring due to the treatment. A definite influence of stress superposition on surface hardness could not be detected. Further investigations regarding plastic deformation due to processing the bended specimens on a curved specimen holder must be carried out to determine the physical effects leading to higher residual stresses. For this, experiments on treatment of only one specimen side or treatment of the first side on a curved holder and second side on a flat holder could be carried out. Furthermore, pre-stress can be induced in other ways than bending to achieve uniaxial pre-stress. Microstructural and surface roughness analyses have to be executed to investigate the influence of stress superposition in mechanical surface treatment.

Acknowledgements

The authors would like to thank N. Kashaev and S. Keller from Helmholtz-Zentrum Geesthacht for their valuable support in the hole drilling method and the analysis of the residual stresses.

References

[1] C. A. Rodopoulos, A. T. Kermanidis, E. Statnikov, V. Vityazev, and O. Korolkov, The effect of surface engineering treatments on the fatigue behavior of 2024-T351 aluminum alloy, Journal of materials Engineering and performance, vol. 16, no. 1, 2007, pp. 30–34.

[2] P. Delgado, Cuesta, J. M. Alegre, and A. Díaz, State of the art of deep rolling, Precision Engineering, vol. 46, 2016, pp. 1–10.

[3] R. K. Nalla, I. Altenberger, U. Noster, G. Y. Liu, B. Scholtes, and R. O. Ritchie, On the influence of mechanical surface treatments—deep rolling and laser shock peening—on the fatigue behavior of Ti–6Al–4V at ambient and elevated temperatures, Materials Science and Engineering: A, vol. 355, 1-2, 2003, pp. 216–230.

[4] N. Kashaev et al., Effects of laser shock peening on the microstructure and fatigue crack propagation behaviour of thin AA2024 specimens, International Journal of Fatigue, vol. 98, 2017, pp. 223–233.

[5] I. Nikitin and I. Altenberger, Comparison of the fatigue behavior and residual stress stability of laser-shock peened and deep rolled austenitic stainless steel AISI 304 in the temperature range 25–600 C, Materials Science and Engineering: A, vol. 465, 1-2, 2007, pp. 176–182.

[6] J. T. Maximov, G. V. Duncheva, A. P. Anchev, and M. D. Ichkova, Slide burnishing—review and prospects, The International Journal of Advanced Manufacturing Technology, vol. 104, 1-4, 2019, pp. 785–801.

[7] J. T. Maximov, A. P. Anchev, G. V. Duncheva, N. Ganev, K. F. Selimov, and V. P. Dunchev, Impact of slide diamond burnishing additional parameters on fatigue behaviour of 2024-T3 Al alloy, Fatigue & Fracture of Engineering Materials & Structures, vol. 42, no. 1, 2019, pp. 363–373.

[8] R. Teimouri, S. Amini, and A. B. Bami, Evaluation of optimized surface properties and residual stress in ultrasonic assisted ball burnishing of AA6061-T6, Measurement, vol. 116, 2018, pp. 129–139.

[9] S. Chatti, M. Hermes, A. Weinrich, N. Ben Khalifa, and A. E. Tekkaya, New incremental methods for springback compensation by stress superposition, International Journal of Material Forming, vol. 2, no. 1, 2009, p. 817.

[10] J. Hu, Z. Marciniak, and J. Duncan, Mechanics of sheet metal forming: Elsevier, 2002.

[11] A. A. García-Granada, G. Gomez-Gras, R. Jerez-Mesa, J. A. Travieso-Rodriguez, and G. Reyes, Ball-burnishing effect on deep residual stress on AISI 1038 and AA2017-T4, Materials and Manufacturing Processes, vol. 32, no. 11, 2017, pp. 1279–1289.

[12] G. S. Schajer, Advances in hole-drilling residual stress measurements, Experimental mechanics, vol. 50, no. 2, 2010, pp. 159–168.

[13] S. Chupakhin, N. Kashaev, and N. Huber, Effect of elasto-plastic material behaviour on determination of residual stress profiles using the hole drilling method, The Journal of Strain Analysis for Engineering Design, vol. 51, no. 8, 2016, pp. 572–581.

[14] D. Olfa, Z. Amna, G. Amen, and N. Rachid, Identification of the anisotropic behavior of an aluminum alloy subjected to simple and cyclic shear tests, Proceedings of the Institution of Mechanical Engineers, Part C: Journal of Mechanical Engineering Science, vol. 233, no. 3, 2018, pp. 911–927.